



Numerical Analysis of the Thermal Influence of Conduction and Contact Thermal Resistance in Multi-Layered Cutting Tool

Rogério Fernandes Brito^{1*}, Ricardo Luiz Perez Teixeira¹, Rafael Thomaz de Camargo Rodrigues¹, José Carlos de Lacerda¹, Tarcísio Gonçalves de Brito¹, Paulo Mohallem Guimarães¹, Henrique Marcio Pereira Rosa² and Júlio César Costa Campos²

¹Instituto de Engenharia Integrada, Universidade Federal de Itajubá, Rua Irmã Ivone Drummond, 200, Distrito Industrial II, 35903-087, Itabira, Minas Gerais, Brasil. ²Laboratório de Sistemas Térmicos, Departamento de Engenharia de Produção e Mecânica, Universidade Federal de Viçosa, Avenida Prof. Peter Henry Rolfs, s/n, 36570-900, Viçosa, Minas Gerais, Brasil. *Author for correspondence. E-mail: rogbrito@unifei.edu.br

ABSTRACT. During the turning process, the cutting tool heats up during use, potentially reaching temperatures above 900°C. When these temperature levels are reached, the cutting tool loses its mechanical properties and wears out prematurely. To address this issue, a solution was found in coating the cutting tool with a thin layer of thermally insulating material. The purpose of this work was to numerically simulate the heating phenomenon in the transient regime of a tool and tool holder set while considering the presence of the coating, as well as to evaluate heat exchange by conduction. Another factor considered in this work was the presence of contact resistance between the tool and the tool holder, which, according to some studies, impacts the temperature field of the cutting tool. Some parameters related to contact resistance were taken into account to make the model closer to real situations. Simulations were carried out using the COMSOL[®] program to solve the transient three-dimensional heat diffusion equation using the Finite Element Method. Subsequently, the temperatures found for the uncoated cutting tool were compared to the temperatures found for the cutting tool coated with Titanium Nitride (TiN), Aluminum Oxide (Al₂O₃), and Titanium Carbide (TiC).

Keywords: Cutting tool; heat transfer; COMSOL[®]; coating; contact resistance.

Received on February 21, 2024.

Accepted on June 11, 2024.

Introduction

The machining process, similar to other processes that perform high material deformations, generates a large amount of heat. Heat significantly influences the tool's performance during this process. Therefore, developing new materials resistant to high temperatures and methods to extend the life of cutting tools is crucial, enabling higher cutting speeds in machining processes and reducing tool replacement costs.

Determining the temperature during cutting is crucial in studying tool performance as it enables the analysis and understanding of factors influencing its wear and lifespan (Borelli et al., 2001). Moreover, there is a significant reduction in the use of lubricants and refrigerants due to their environmental impact and increased machining costs, highlighting the need for further studies in this thermal area (Tonshoff et al., 2000 and Yen et al., 2004).

Another way to increase tool life is to coat the tool's cutting surface with materials with thermal insulation characteristics that provide less wear on the tool. Coatings for cutting tools were developed to combine wear resistance and toughness. New coating materials have been developed, and their improved performance can be attributed to their thermal characteristics. Hence, investigating the thermal influence of these coatings on cutting tools is important. Hunt and Santhanam (1990) reported that productivity was two to three times higher with coated tools compared to uncoated tools in the turning process.

This study proposes to examine the thermal influence of these coatings on cemented carbide cutting tools. The coating is modeled as a thin layer on top of the cutting tool in a three-dimensional numerical model. With defined boundary conditions and known heat flux from existing literature-based data, the temperature field in the cutting tool can be determined.

Extensive work has been done to find these solutions. Song et al. (2017) analyzed the variation of the cutting temperature in machining with a cemented carbide tool in two cases, one with the tool coated with Ti-MoS₂/Zr composite and the other using the tool without coating.

Using a different composite for the coating, TiAlN/AlCrN, Ghani et al. (2016) studied the wear process that occurs in the cutting tool, analyzing the cases of coated and uncoated tools.

The use of coatings remains the most efficient solution, according to Grzesik (2006). In his work, three composites that have good characteristics and applicability for cutting tool coatings were considered, namely Titanium Nitride (TiN), Titanium Carbide (TiC), and Alumina Oxide (Al_2O_3). Furthermore, several works treat these coatings with these composites.

Zhang and Liu (2017) analyzed the temperature distribution in steady state and transient in cemented carbide cutting tools with a coating layer, such as TiN, TiC, and Al_2O_3 . According to the results obtained, the tool with Al_2O_3 composite coating is the most effective in reducing heat conduction during the machining process.

A study conducted by Zhang et al. (2017) showed a new prediction model that predicts the temperature distribution on the cutting face of a tool with a coating layer based on heat source theory. The authors concluded that the two coated tools generated lower temperatures on the cutting face compared to the uncoated tool, proving the coating's efficiency in prolonging tool life.

Jin et al. (2018) developed a heat partition model for a cutting tool using the finite element method to study the heat conduction mechanism in the secondary strain zone. The authors conducted cutting experiments with tools coated with four different materials: TiC, TiN, TiAlN, and Al_2O_3 . They compared the temperatures obtained on the cutting face for each type of coating.

Ferreira et al. (2018) used the numerical analysis of the influence of coatings on a cutting tool using the COMSOL[®] software and an inverse nonlinear problem. TiN and Al_2O_3 were used as the coating materials for the study. The research was conducted using numerical methods due to the limitations of experimental methods in determining the temperature on the tool surface. The heat flux was estimated using COMSOL[®] and was later compared with previous work by Brito et al. (2009). Ferreira et al. (2018) concluded that the best results were with the Al_2O_3 coating.

Paula et al. (2019) conducted a study to evaluate the performance of a hard metal tool coated through the PVD (Physical Vapor Deposition) and CVD (Chemical Vapor Deposition) processes, during the turning of a hardened martensitic steel AISI 410 subjected to MQL conditions and dry machining. A hard metal tool coated with TiSiN-TiAlN by the PVD process, and another hard metal tool coated with Al_2O_3 , TiC, and TiN by the CVD process were used. The results showed that the Al_2O_3 coating reduces thermal conductivity, resulting in less heat reaching the substrate of the cutting tool.

Zhang et al. (2021) proposed an analytical model to estimate the temperature in a hard metal insert coated with TiN during the turning of a hardened H13 steel sample. To determine the temperature, the authors used the one-dimensional Fourier heat conduction model and the one-dimensional non-Fourier heat conduction model. A K-type thermocouple was embedded in the insert, at a distance of 2 mm from the contact area between the chip and the insert to measure the temperature during the experiments. The results indicated that the discrepancy between the temperature calculated by the non-Fourier transient model and the experimentally measured temperature was less than 12%.

Zhang et al. (2022), building on the work of Zhang et al. (2021), investigated the impact of the material and thickness of the coating on the temperature distribution in hard metal coated inserts. For the analysis, the authors used inserts coated with a single layer (TiN, TiAlN, and Al_2O_3) and multi-layer coated inserts (TiN/TiC/TiN and TiAlN/TiN). An equivalent approximation was used to calculate the thermal conductivity and equivalent thermal diffusivity of the materials in the multi-layer coatings. The results indicated that the temperature in the insert decreases as the thickness of the coating increases, giving the same material. Regarding the coating materials, the lowest temperature in the insert was achieved with the Al_2O_3 coating, due to its lower thermal conductivity.

When two solid bodies with different temperatures come into contact, there is a transfer of heat from the hotter body to the colder one. However, this interaction between the two bodies is not perfect, which can result in a decrease in temperature at the contact interface between them. The existence of a contact resistance between the two surfaces is primarily due to the effects of roughness. This phenomenon is known as thermal contact resistance.

Mondelin et al. (2013) developed a numerical/experimental method to calibrate the contact resistance between the cutting tool and the tool holder during the turning process. They used a laser to heat an uncoated hard metal cutting tool and K-type thermocouples to measure the temperature. Based on the results, they obtained a contact resistance value around the insert of $630 \text{ mm}^2 \cdot ^\circ\text{C}/\text{W}$, which was used to calibrate the simulation.

Norouzifard and Hamed (2014) employed a numerical and experimental approach to calculate the average thermal conductance of contact, which is the reciprocal of contact resistance, in the contact region between the chip and the tool during machining. The temperature in the cutting tool and the heat flow were determined using a thermal inversion methodology. The results revealed that the value of Thermal Contact Conductance (TCC) is directly proportional to the thermal conductivity of the machined material and inversely proportional to its mechanical resistance.

Mathieu et al. (2015) developed a 3D numerical model to simulate the thermal gradient during turning. They used the method described by Mondelin et al. (2013) to calibrate the contact resistance between the cutting tool, shim, and tool holder. The authors determined a contact resistance between the shim and the tool holder of $180 \text{ mm}^2 \text{ }^\circ\text{C/W}$. For the contact resistance between the cutting tool and other elements (shim and fixing screw), the obtained value was $200 \text{ mm}^2 \text{ }^\circ\text{C/W}$.

Xian et al. (2018) conducted a review of the most commonly used experimental techniques to characterize Thermal Contact Resistance (CTR): steady-state method, T-type method, micro-thermometry, Raman-based techniques, infrared thermography measurements, laser-flash measurements, photoacoustic techniques, 3ω method, and transient thermo-reflectance techniques. The authors concluded that although some techniques have proven their reliability, all have their areas of application and limitations. Despite most of the studied techniques being performed at room temperature, the authors highlighted that CTR is influenced by extreme conditions such as high temperatures or high pressures.

Hao and Liu (2019) performed dry cut tests with H13 hardened steel using a TiAlN composite coating, including Contact Thermal Resistance (CTR) among the parts of the assembly.

Thus, we used computational tools in CAD and CAE in the present work, in which the heat flux adopted was obtained from Carvalho et al. (2006). Nonlinear thermal properties were defined and determined from adjustment equations as a function of temperature as described by Incropera et al. (2011). The temperature-dependent thermophysical properties adopted in the models, with the exception of the emissivity and the temperature-dependent thermal property values of 1045 steel, the tool holder material, were obtained from Grzesik et al. (2009). Cemented carbide tool emissivity values varying with temperature were obtained from the work of Jiang et al. (2016).

Figure 1 shows the unstructured finite element mesh in the contact area at the typical chip-tool interface used in the numerical simulations of the present work with an area of approximate value of 1.424 mm^2 . This area was obtained experimentally by Carvalho et al. (2006).

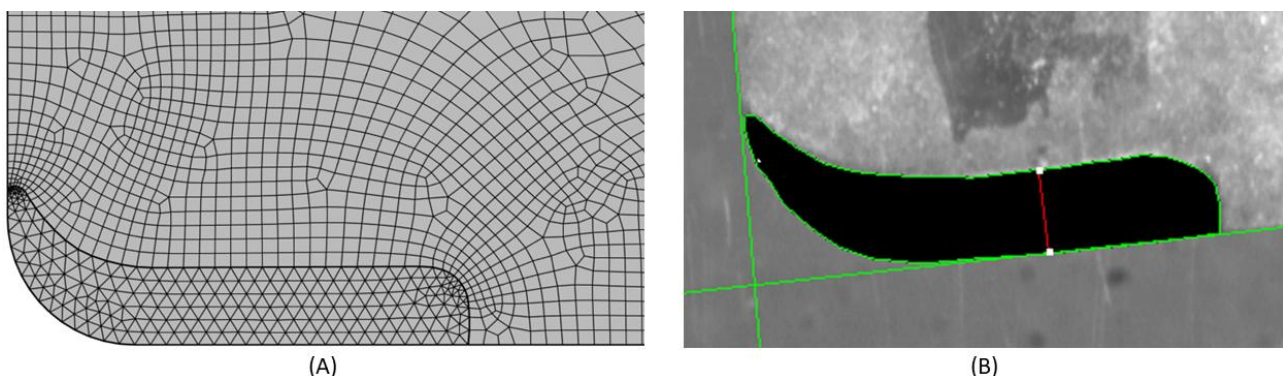


Figure 1. Unstructured finite element mesh of the tool of this work, being (a) a partial detail of the heat flux region and (b) a video image of the contact area at the chip-workpiece-tool interface (Carvalho et al., 2006).

To model the natural convection heat transfer coefficient varying with temperature, the COMSOL® software uses the empirical correlations of Incropera et al. (2011). For the numerical validation of the present work, an average value of the convective heat transfer coefficient equal to $20 \text{ W m}^{-2} \text{ K}$ was chosen, according to Carvalho et al. (2006). Furthermore, in the present work, the TCR between the parts of the tool was implemented based on experimental data from Corrêa Ribeiro et al. (2022) and is available in the COMSOL® package. The following parameters were necessary to obtain: the inclusion of the micro-hardness of the tool, the cutting force, and the clamping force of the clamp, which holds the cutting tool together, considering only one coating material.

Materials and methods

Thus, the present work, in addition to the implementation of TCR and the natural convection coefficient, presented an improvement over previous works by the present authors, considering the numerical simulation with multiple coating layers on the tool to seek a more realistic model.

Problem description

The numerical thermal model used in this work was a carbide cutting tool, a tool holder, and a shim, based on the experimental and numerical work of Carvalho et al. (2006). Two analyses were carried out. In the first analysis, only the uncoated cemented carbide tool was considered, and in the second analysis the tool having multi-layer coating was considered. From these two models, numerical simulations were carried out to analyze the effect of the coating on the temperature field that forms on the tool during the machining process. Shown below are the main dimensions in mm of the substrate of the cemented carbide cutting tool (Figure 2a), the tool holder (Figure 2b), and the shim (Figure 2c) used in the models.

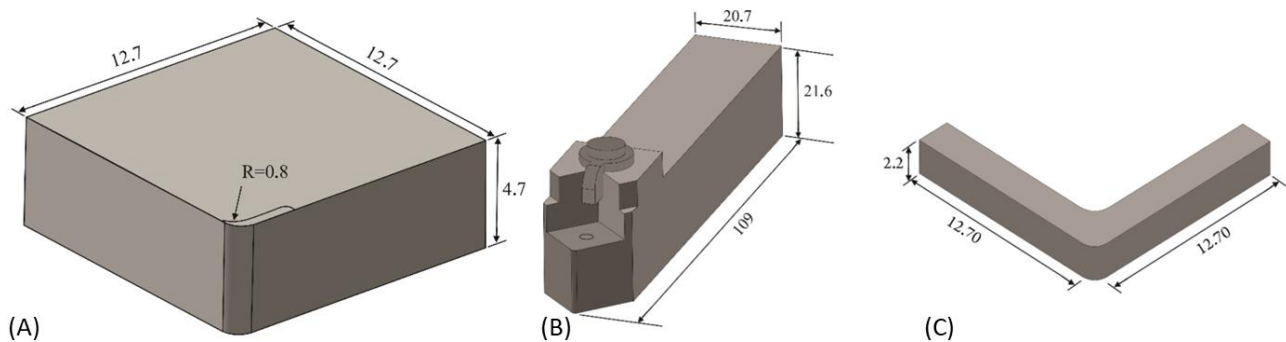


Figure 2. Main dimensions (mm): (a) cemented carbide cutting tool, (b) tool holder, and (c) shim.

Figure 3a shows a portion of the coating detailing the contact area between the cutting tool and the part, represented in yellow. To illustrate the differences between the two models studied, both models were divided into domains: cemented carbide cutting tool substrate (Ω_1), shim (Ω_2), tool holder (Ω_3), TiC coating (Ω_4), Al_2O_3 coating (Ω_5), and TiN coating (Ω_6) (Grzesik, 2006).

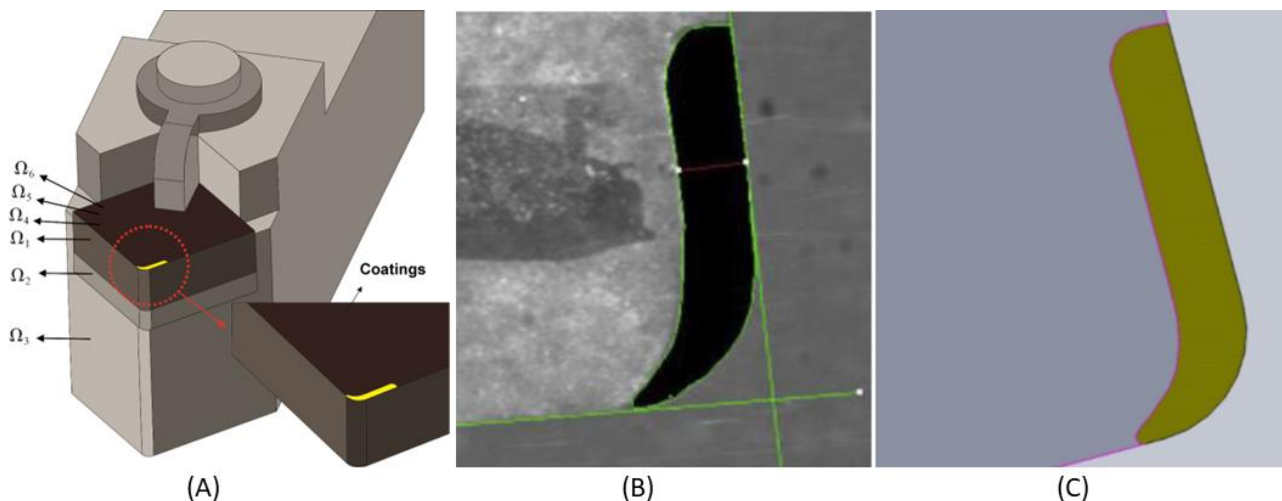


Figure 3. (a) Assembly of the tool and tool holder set and detail of the coatings. Comparison between the contact areas of the cutting tool: (b) experimental and (c) numerical in this work.

The contact region between the cutting tool and the part, which is shown in Figure 3a in yellow color, was modeled considering the experimental measurement made by Carvalho et al. (2006) using an image analyzer. In Figure 3b and Figure 3c, the region measured experimentally (Figure 3b) is compared with the region S_1 of the numerical model (Figure 3c) of the present work.

The temperature-dependent thermophysical properties adopted in the present work, with the exception of emissivity, and the temperature-dependent thermal tool holder material property values of 1045 steel were

taken from the work of Grzesik et al. (2009). Cemented carbide tool emissivity values varying with temperature were obtained from the work of Jiang et al. (2016).

In this work, thermal radiation is also considered in the simulation of the models, necessitating knowledge of the emissivity values of the materials. Numerical data obtained from the convective heat transfer coefficient of Carvalho et al. (2006) and Incropera et al. (2011) were used. Cemented carbide tool emissivity values, considering temperature variation, were obtained from the work by Jiang et al. (2016).

The emissivity of TiN, Al₂O₃, and 1045 steel was taken from the studies by Yuste et al. (2010), Wang et al. (2013), and Polozine and Schaeffer (2005), and their values were respectively equal to 0.2, 0.85, and 0.83. In the case of TiC emissivity, 0.2 was adopted in the present work.

Some hypotheses were adopted in the two proposed models, such as perfect thermal contact between the coating and the substrate; emissivity of constant materials, in relation to temperature, for the coating and tool holder; and constant ambient temperature and absence of internal heat generation in all domains that were studied.

The resolution of the thermal problem presented in this work was done using the direct method to obtain the numerical temperature values since all boundary conditions were already known. The governing equations of the studied physical problem are shown below.

Thermal model

The equation that describes the thermal model used is the transient three-dimensional heat diffusion equation (Equation 1), considering variable properties with temperature:

$$\frac{\partial}{\partial x} k(T) \frac{\partial T}{\partial x}(x, y, z, t) + \frac{\partial}{\partial y} k(T) \frac{\partial T}{\partial y}(x, y, z, t) + \frac{\partial}{\partial z} k(T) \frac{\partial T}{\partial z}(x, y, z, t) = \rho c_p(T) \frac{\partial T}{\partial t}(x, y, z, t). \quad (1)$$

Subject to the convection and radiation boundary condition (Equation 2):

$$-k(T) \frac{\partial T}{\partial \eta}(x, y, z, t) = h(T)(T - T_{\infty}) + \sigma \varepsilon(T)(T^4 - T_{\infty}^4). \quad (2)$$

In the area of contact between the tool and the workpiece, the boundary condition is imposed transient heat flux (Equation 3):

$$-k(T) \frac{\partial T}{\partial z}(x, y, 0, t) = q_0''(t) \text{ em } S_1. \quad (3)$$

The initial condition of the model used for all domains is given by (Equation 4):

$$T(x, y, z, 0) = T_0. \quad (4)$$

Numerical method

All numerical simulations in this work were performed using the commercial program COMSOL® Multiphysics 5.4, which uses the finite element method. In the case of heat transfer problems in transient solids, COMSOL® uses the BDF (backward differentiation formula) method to approximate the time derivatives and the GMRES (generalized minimum residual) method, being an iterative method for the resolution of general linear systems in the formula $Ax = b$.

In the case of modeling the natural convection coefficient varying with temperature, COMSOL® uses the empirical correlations of Incropera et al. (2011) that are already implemented in this computational package.

On all surfaces, air was considered the surface contact fluid with an external ambient temperature of 29.2°C and an absolute pressure of 1 atm.

Experimental procedure

One of the main difficulties in analyzing a machining process through a thermal look is knowing the precise heat flow at the contact interface between the part and the cutting tool. Experimental tests are necessary to obtain the thermal field in the set. The present work used experimental and numerical temperature and transient heat flux data from Carvalho et al. (2006). This heat flux is used in the present work as a boundary condition applied in area S_1 (Figure 3c). Figure 4 shows the positions of the sensors, which are used by Carvalho et al. (2006), in order to obtain the temperature field and verify the thermal influence of multilayer coatings.

The cutting parameters used in this work were the following: 0.138 mm feed/revolution; cutting speed of 135.47 m/min; initial diameter of 77.0 mm; machined length of 77.0 mm; 5.0 mm cutting depth; and 580.0 rpm rotation (Carvalho et al., 2006).

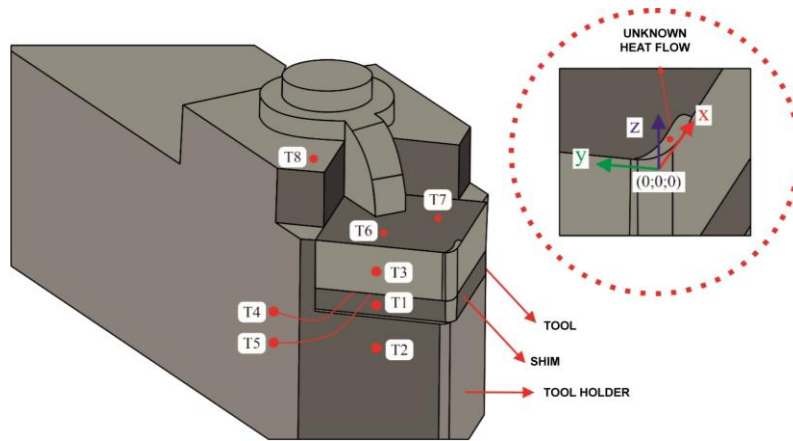


Figure 4. Positioning thermocouples T₁ to T₈ in the tool set, shim, and tool holder.

Contact thermal resistance (CTR)

In composite systems with two or more materials or parts, there may be an abrupt drop in temperature at the interface between the materials due to imperfect contact between them (Incropera et al., 2011).

In the present work, the analysis of the thermal contact resistance (TCR) was considered based on data obtained from Corrêa Ribeiro et al. (2022). The TCR is extensively present in any assembly and modifies the heat conduction pattern as it occurs in electronic circuits, among other equipment (Corrêa Ribeiro et al., 2022).

For the COMSOL® software to calculate the contact resistance, it was necessary to collect the data used as parameters between any two domains from the literature, namely: the convective heat transfer coefficient present in the air-filled interstices, *hg*; mean surface roughness, *σasp*; slope of roughness peaks, *masp*; softer surface hardness, *Hc*; and contact pressure, *P*. In this work, the values adopted for the required parameters were taken from the work of Corrêa Ribeiro et al. (2022).

Obtaining temperature profiles

In addition to using thermocouples to analyze the temperature at various points on the tool and the tool holder, numerical probes were inserted along the cutting tool and positioned according to the coordinates indicated in Table 1 in both cases analyzed.

Table 1. Coordinates of numerical probes.

Probe	R00	R01	R02	R03	R04	R05	R06	R07	R08	R09	R10
x [mm]	0.25	0.25	0.25	0.25	0.25	0.25	0.25	0.25	0.25	0.25	0.25
y [mm]	1.35	1.35	1.35	1.35	1.35	1.35	1.35	1.35	1.35	1.35	1.35
z [mm]	0.000	-0.001	-0.002	-0.003	-0.004	-0.005	-0.006	-0.007	-0.008	-0.009	-0.010

The probes are evenly distributed over the first 10 μm, which is the thickness of the coating adopted. Next, a schematic drawing is presented in Figure 5 to better explain the placement of the numerical probes along the set.

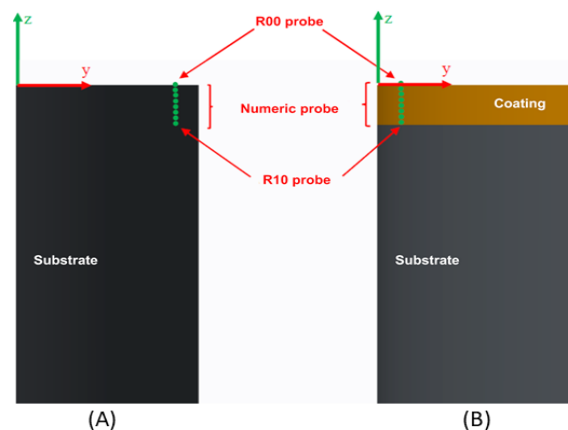


Figure 5. Positioning, without scaling, of the numerical probes in the uncoated (a) and coated (b) model. Source: adapted from Corrêa Ribeiro et al. (2022).

In Figure 5, the R00 probe is positioned to calculate the temperatures on the tool exit surface, that is, in the region that would be the interface between the chip and the cutting tool in a real model. The R10 probe is located 10 μm below the exit surface, being the point equivalent to the interface between the coatings and the substrate in the cases that consider the coatings. This distribution is adopted in both cases with and without coating to investigate the thermal influence of different thermal properties and different materials.

Results

Numeric model validation

To validate the numerical methodology implemented in this work, numerical simulations of the thermal influence of the mesh refinement were performed, using the commercial package COMSOL® Multiphysics 5.4. Used in this numerical analysis were experimental data from Carvalho et al. (2006), considering an ISO K10 cemented carbide cutting tool with dimensions 12.7 mm x 12.7 mm x 4.7 mm with thermophysical properties (Figure 6): $k = 43.1 \text{ W m}^{-1} \text{ K}^{-1}$, $c_p = 332.94 \text{ J kg}^{-1} \text{ K}^{-1}$ e $\rho = 14,900.00 \text{ kg m}^{-3}$.

In his laboratory-controlled experiment, Carvalho et al. (2006) placed a resistive heater, a heat flux transducer, and two thermocouples on the cutting tool in which all sensors were calibrated. The resistive heater was connected to a direct current source, providing heat generation through the Joule effect. The heat flux transducer, positioned between the heater and the tool, measured the thermal flux supplied to the cutting tool. Cutting tool temperatures were measured from two thermocouples connected to a computer-controlled Agilent 34980A data acquisition system.

In the isolated cutting tool (Figure 6), there are two thermocouples for calculating the temperature: thermocouple 1 at point $x = 3.5 \text{ mm}$, $y = 8.9 \text{ mm}$, and $z = 4.7 \text{ mm}$; and thermocouple 2 at point $x = 6.5 \text{ mm}$, $y = 5.9 \text{ mm}$, and $z = 4.7 \text{ mm}$.

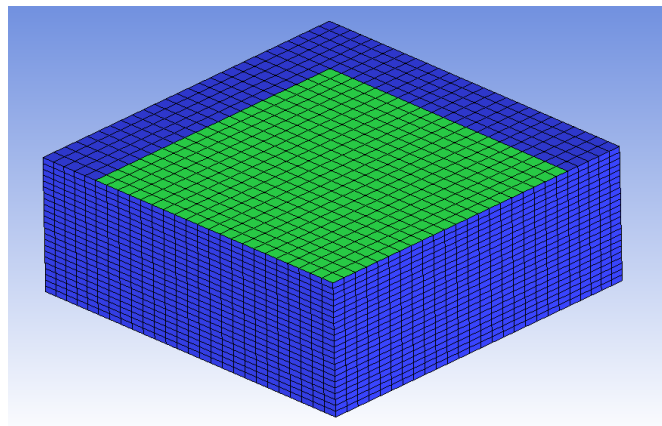


Figure 6. Cutting tool isolated.

In this work, three computational meshes were generated to study the independence of the mesh on the obtained temperature results: 'coarser,' 'normal,' and 'finer,' which are refinements pre-defined in the COMSOL® simulation software. Table 2 and Table 3 show the results of the deviations with variations in the number of elements, number of nodes, for each thermocouple. The number of elements and nodal points was obtained in COMSOL® itself through a function called "statistics." The deviation was found using the formula $\text{Deviation} = (T_{\text{num}} - T_{\text{exp}})/T_{\text{exp}} \cdot 100$, where T_{num} is the numerical temperature obtained in the present work using the flow measured in the laboratory by Carvalho et al. (2006) and T_{exp} is the experimental temperature collected in a controlled experiment (Carvalho et al., 2006).

Table 2. Study of the thermal influence of the grids on the temperature obtained from thermocouple T₁.

Tetrahedral mesh	Number of elements	Number of nodal points	Deviation [%]
Mesh 1 (Coarser)	897	423	4.74
Mesh 2 (Normal)	1396	513	4.73
Mesh 3 (Finer)	3390	996	4.15

Table 3. Study of the thermal influence of the grids on the temperature obtained from thermocouple T₂.

Tetrahedral mesh	Number of elements	Number of nodal points	Deviation [%]
Mesh 1 (<i>Coarser</i>)	897	423	8.78
Mesh 2 (<i>Normal</i>)	1396	513	8.78
Mesh 3 (<i>Finer</i>)	3390	996	8.17

From the tables, it was verified that the 'normal' mesh deviation was 4.73%, considered satisfactory compared to the more refined mesh, which was 4.15%. Thus, the 'normal' mesh was used to validate the numerical methodology.

Figure 7 shows the experimental thermal flux measured by Carvalho et al. (2006), ranging from t = 0 to 110 s. Figure 8a and Figure 8b below, obtained by thermocouples T₁ and T₂, presents the experimental temperature curves by Carvalho et al. (2006) and the numerical temperatures obtained by the present work, in which COMSOL® was used.

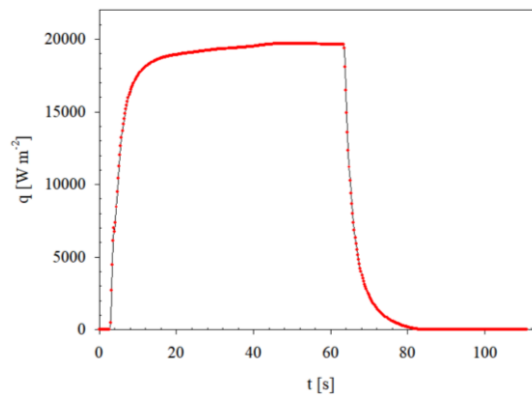


Figure 7. Experimental thermal flow (Carvalho et al., 2006).

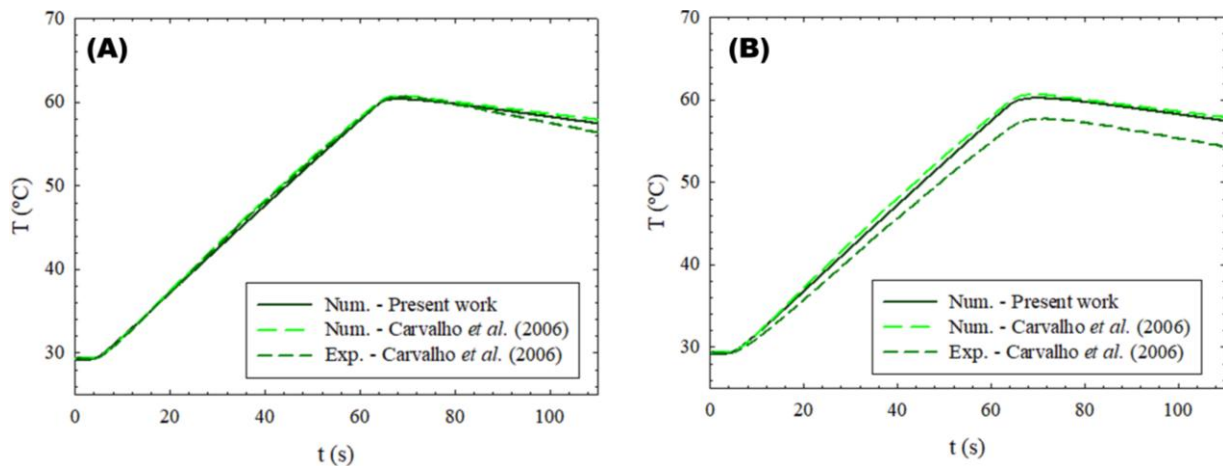


Figure 8. Thermocouples T₁ (a) and T₂ (b): comparison between the numerical temperatures calculated in this work and the experimental and numerical temperatures (Carvalho et al., 2006).

In Figure 8a and Figure 8b, the greatest deviation found for thermocouple T₁ at 109.67 seconds was 4.73%, and for thermocouple T₂ at 109.67 seconds, it was 8.78%. Thus, the numerical result in COMSOL® was satisfactory for the direct problem where the input is known and the output is obtained.

Analysis of temperature variation between thermocouples and numerical probes comparing cases with and without coating

In many dynamic heat transfer situations, such as in a machining process, surface temperature profiles on a hard-to-reach solid or the heat flux need to be determined. Normally, these surface temperatures are obtained from temperature measurements in one or more locations where there is access to the medium. This is called the inverse problem. In a system, an inverse problem is characterized when the output is known and the input needs to be estimated.

The numerical results obtained in this work were compared with the experimental and numerical results from Carvalho et al. (2006) and the numerical results from Corrêa Ribeiro et al. (2022), both referenced in Figure 9a and Figure 9b, respectively, considering the uncoated cutting tool.

In Section 3.1, “Validation of the Numerical Model,” the implemented numerical methodology was validated. The study utilized experimental data from Carvalho et al. (2006), which involved controlled laboratory experiments with a cemented carbide cutting tool of dimensions 12.7 mm x 12.7 mm x 4.7 mm. The heat flow area for this isolated cutting tool in the laboratory was 10.4 mm x 10.4 mm.

Results showing deviations relative to the number of elements and nodes for each thermocouple were presented in Table 2 and Table 3. These values were obtained directly in COMSOL® using the “statistics” function. The formula for calculating deviation was $\text{Deviation} = (T_{\text{num}} - T_{\text{exp}})/T_{\text{exp}} \cdot 100$, where T_{num} is the numerical temperature based on the flow measured in the lab by Carvalho et al. (2006), and T_{exp} is the experimental temperature from controlled experiments. A deviation of 4.73% was observed with the “normal” mesh, which was considered satisfactory compared to the more refined mesh’s deviation of 4.15%. Therefore, the “normal” mesh was employed to validate the numerical methodology.

Considering the thermal influence of computational mesh refinement on the isolated cutting tool, a similar mesh configuration, generated by COMSOL® Multiphysics r. 6.0, was adopted for the assembly comprising the cutting tool, shim, and tool holder. If further details or assistance are required, please inquire.

Data estimated numerically by Carvalho et al. (2006) of the transient heat flux in the cutting tool set, shim, and tool holder through their study of the inverse problem were used in the present work as input data in the COMSOL® package.

Next, the numerical results of the temperatures in each thermocouple and in the analyzed numerical probes, obtained in the present work for the set of cutting tool, shim, and tool holder, are presented and analyzed.

First, the case results for the uncoated assembly are presented. Figure 9a shows the temperature results for the eight numerical probes inserted via the COMSOL® package analyzed in the same positions as the thermocouples used in the work by Carvalho et al. (2006). Figure 9b shows the results of the temperature values for the 11 numerical probes placed in the cutting tool and workpiece contact region, for a depth of up to 10 μm , considering the same positions of the numerical probes used in Corrêa Ribeiro et al.’s work (2022).

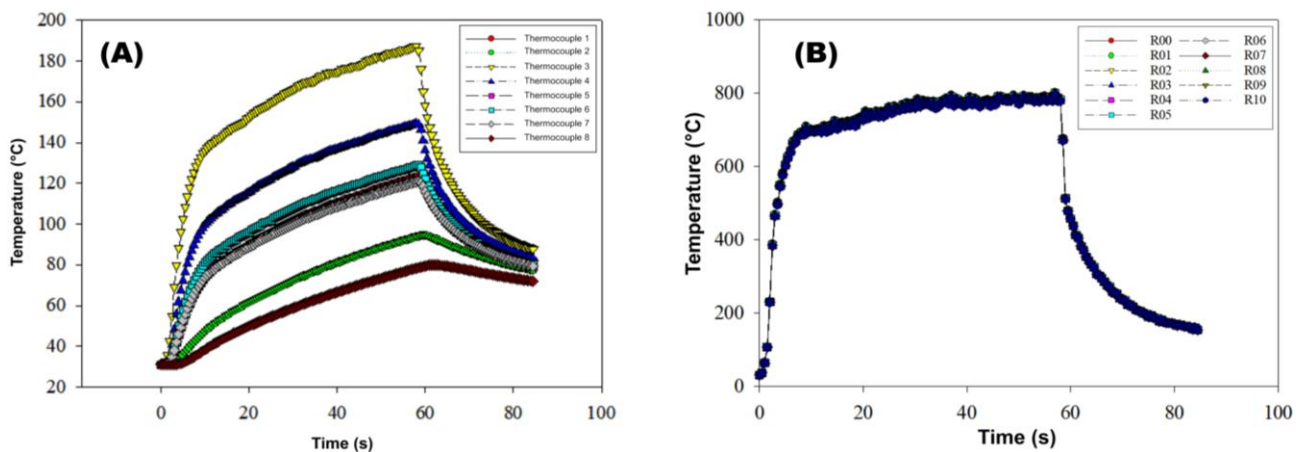


Figure 9. (a) Thermocouple temperature comparison in the uncoated case. (b) Comparison of the temperature of the 10 probes in the uncoated case.

Figure 10a and Figure 10b present the numerical results obtained from the present work, respectively, according to the experimental and numerical results from Carvalho et al.’s (2006) work and numerical results from Corrêa Ribeiro et al.’s work (2022), considering the presence of the 10 μm coating.

In the current study, for the case with multilayer coating, an 18-core Intel Xeon® E5-2686v4 processor with 32 GB of ECC RAM was utilized, consuming 35 minutes and 6 seconds of CPU processing time. This was for a computational mesh with tetrahedral elements, unstructured mesh, comprising 36,368 elements and 150,185 nodal points across the entire assembly of the cutting tool, shim, and tool holder.

The results of the case considering the three coating layers are shown in Figure 10a and Figure 10b, in which it is possible to observe that the temperature variation becomes greater due to the use of these coatings. This result is relevant, showing that coatings retain more heat on the upper face of the tool thereby preventing it from passing to the substrate and can reduce tool life.

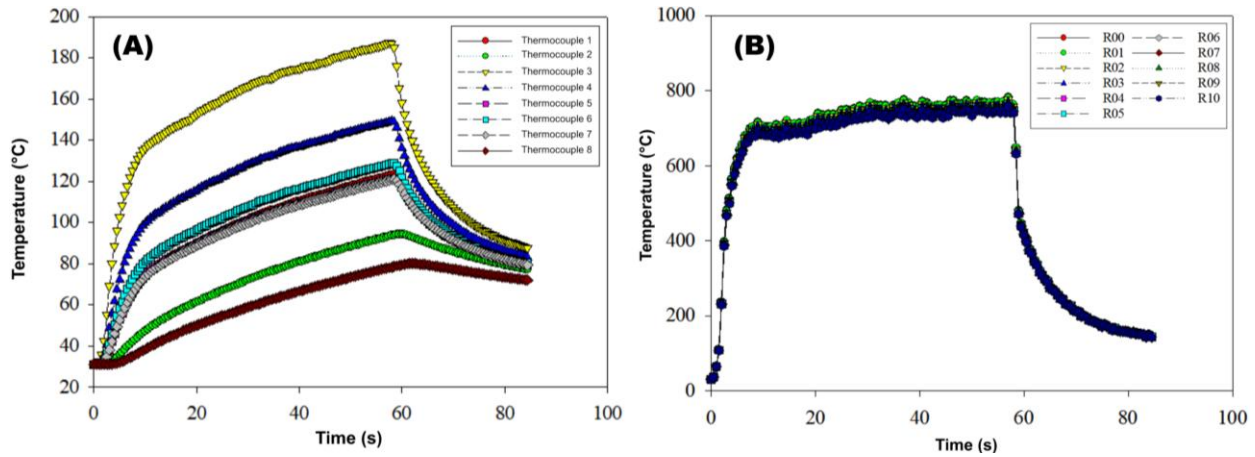


Figure 10. (a) Thermocouple temperature comparison in the case with 3 coating layers. (b) Comparison of the temperature of the 10 probes in the case with coating.

To compare the analyzed thermocouples, the graphs in Figure 11a, 11b, and 11c below were plotted, which respectively refer to the comparisons of the temperatures of thermocouples T_3 , T_6 , and T_7 .

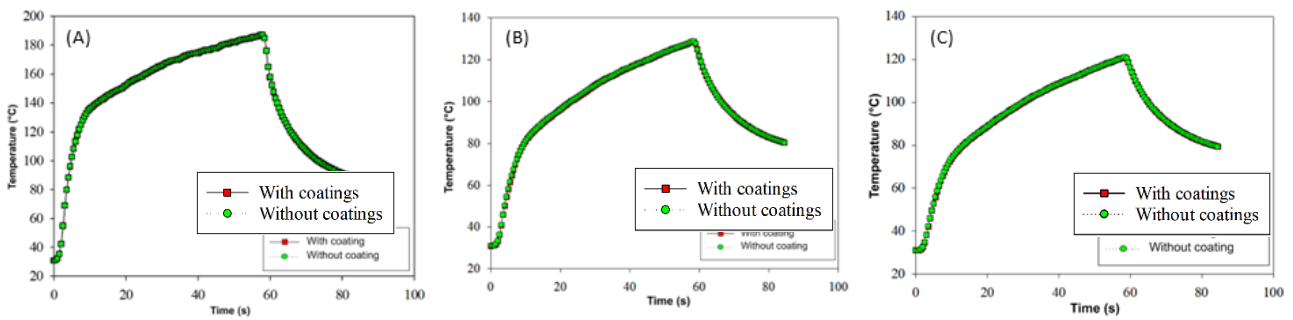


Figure 11. (a) Comparison of T_3 thermocouple temperatures. (b) Comparison of T_6 thermocouple temperatures. (c) Comparison of T_7 thermocouple temperatures.

Analyzing these comparisons between the temperatures of these three thermocouples from (Figure 11a, 11b, and 11c) of the present work, a relevant result was not perceived as observed in the analysis of the numerical probes used inside the coating, as was performed in the work of Corrêa Ribeiro et al. (2022). For this reason, the results of the probes started to be observed with more attention, and that is why a comparison of the values of the probes in both cases of this study was made with the values of the probes analyzed by Corrêa Ribeiro et al. (2022).

Figure 12 illustrates this comparison. Through this comparison, it was possible to better observe the thermal influence of the presence of coatings by this method of analysis to reduce the heat transfer from the contact area to the rest of the cutting tool.

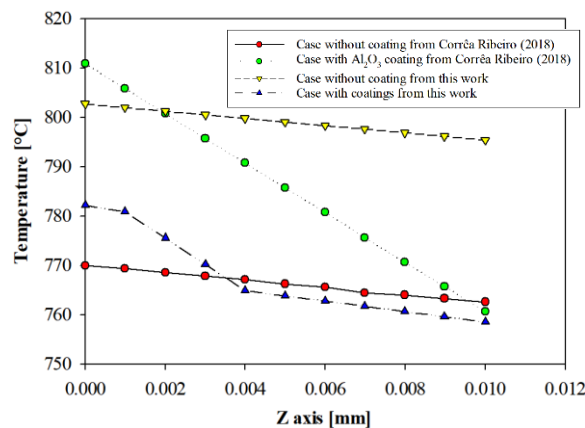


Figure 12. Comparison of coating temperatures, calculated in numerical probes of the present work, for $t = 57$ s, between this work and the work by Corrêa Ribeiro et al. (2022).

Also, with respect to Figure 12, it was observed that, in addition to the case considering an Alumina (Al_2O_3) coating by Corrêa Ribeiro et al. (2022), the case of this work that considered multilayer coatings with TiN, Al_2O_3 , and TiC materials presented a greater temperature variation along the numerical probes.

According to the results obtained, it is also possible to notice a variation of approximately 23.64°C between the R00 probe and the R10 probe Figures 5 and 12, in this case considering a multilayer coating of TiN, Al_2O_3 , and TiC with a thickness of $10\ \mu\text{m}$.

It can also be observed that the region of the blue curve in Figure 12, which comprises the elevation of $z = -0.001\ \text{mm}$ to $z = -0.004\ \text{mm}$ and represents the region of the coating of Alumina Oxide (Al_2O_3) material, had a drop similar to the drop in temperature of Corrêa Ribeiro et al. (2022), who used a coating of only Al_2O_3 , represented by the green curve in the graph. In the case of Corrêa Ribeiro et al. (2022), the temperature drop was 51.55°C considering only a single $10\ \mu\text{m}$ -thick Al_2O_3 coating. For the case without coating, the temperature reduction in $10\ \mu\text{m}$ of thickness in the cutting tool for the present work and for the work of Corrêa Ribeiro et al. (2022) was, respectively, 7.30 and 7.46°C .

Conclusion

The following conclusions can be presented in relation to the numerical results obtained for the thermal model of heat transfer in coated and uncoated cutting tools:

- The results of the present work were in agreement with the numerical results obtained by Corrêa Ribeiro et al. (2022);
- The studies carried out showed that for a uniform heat source with time variation, considering a surface of constant contact between the chip and the tool, the temperature in the tool is directly influenced by the coatings when the thermal properties of the coating are different from those of the substrate, even for a thin coating of $10\ \mu\text{m}$;
- The coating layer deposited on the analyzed cemented carbide tool presented satisfactory results during the continuous cutting process. A variation of approximately 24°C (point A) was observed between the numerical probes under analysis in the case considering the multilayer coatings (TiN, Al_2O_3 , and TiC); and
- The present analysis of heat transfer in multilayer coated carbide cutting tools revealed promising characteristics in the study of tool life, cost reduction in dry machining processes, reduction of time spent in the study of thermal influence coatings, and reduction in the number of experiments. These characteristics are also validated in other works such as Kusiak et al. (2005) and Marusich et al. (2002).

References

- Borelli, J. E., França, C. A., Medeiros, C. F., & Gonzaga, A. (2001). Análise da temperatura na região de contato entre a peça e a ferramenta. *Revista Máquinas e Metais*, 114–125.
- Brito, R. F., Carvalho, S. R., Lima e Silva, S. M. M., & Ferreira, J. R. (2009). Thermal analysis in coated cutting tools. *International Communications in Heat and Mass Transfer*, 36(4), 314–321. <https://doi.org/10.1016/j.icheatmasstransfer.2009.01.004>
- Carvalho, S. R., Lima e Silva, S. M. M., Machado, A. R., & Guimarães, G. (2006). Temperature determination at the chip-tool interface using an inverse thermal model considering the tool and tool holder. *Journal of Materials Processing Technology*, 179, 97–104. <https://doi.org/10.1016/j.jmatprotec.2006.05.014>
- Corrêa Ribeiro, C. A., Ferreira, J. R., & Lima e Silva, S. M. M. (2022). Thermal influence analysis of coatings and contact resistance in turning cutting tool using COMSOL. *The International Journal of Advanced Manufacturing Technology*, 118(1-2), 275–289. <https://doi.org/10.1007/s00170-021-07835-4>
- Ferreira, D. C., Magalhães, E. S., Brito, R. F., & Lima e Silva, S. M. M. (2018). Numerical analysis of the influence of coatings on a cutting tool using COMSOL. *International Journal of Advanced Manufacturing Technology*, 97(1–4), 1305–1314. <https://doi.org/10.1007/s00170-018-2017-6>
- Ghani, J. A., Che Haron, C. H., Kasim, M. S., Sulaiman, M. A., & Tomadi, S. H. (2016). Wear mechanism of coated and uncoated carbide cutting tool in machining process. *Journal of Materials Research*, 31(13), 1873–1879. <https://doi.org/10.1557/jmr.2016.204>
- Grzesik, W. (2006). Determination of temperature distribution in the cutting zone using hybrid analytical-FEM technique. *International Journal of Machine Tools and Manufacture*, 46, 651–658. <https://doi.org/10.1016/j.ijmachtools.2005.08.004>

- Grzesik, W., Nieslony, P., & Bartoszek, M. (2009). Modeling of the cutting process: Analytical and simulation methods. *Advances in Manufacturing Science and Technology*, 33, 5–29.
- Hao, G., & Liu, Z. (2019). Experimental study on the formation of TCR and thermal behavior of hard machining using TiAlN coated tools. *International Journal of Heat and Mass Transfer*, 140, 1–11. <https://doi.org/10.1016/j.ijheatmasstransfer.2019.05.019>
- Hunt, J. L., & Santhanam, A. T. (1990). Coated carbide metal cutting tools: Development and applications. In *The Winter Annual Meeting of The American Society of Mechanical Engineers* (Vol. 25–30, pp. 139–155).
- Incropera, F. P., DeWitt, D. P., Bergman, T. L., & Lavine, A. (2011). *Fundamentals of heat and mass transfer* (7th ed.). John Wiley & Sons.
- Jiang, F., Zhang, T., & Yan, L. (2016). Estimation of temperature-dependent heat transfer coefficients in near-dry cutting. *International Journal of Advanced Manufacturing Technology*, 86, 1207–1218. <https://doi.org/10.1007/s00170-015-8213-1>
- Jin, D., Jingjie, Z., & Ligu, W. (2018). Heat partition and rake face temperature in the machining of H13 steel with coated cutting tools. *International Journal of Advanced Manufacturing Technology*, 94(9–12), 3691–3702. <https://doi.org/10.1007/s00170-017-1158-y>
- Kusiak, A., Battaglia, J. L., & Rech, J. (2005). Tool coatings' influence on the heat transfer in the tool during machining. *Surface and Coatings Technology*, 195, 29–40. <https://doi.org/10.1016/j.surfcoat.2004.06.036>
- Marusich, T. D., Brand, C. J., & Thiele, J. D. (2002). A methodology for simulation of chip breakage in turning processes using an orthogonal finite element model. In *Proceedings of the Fifth CIRP International Workshop on Modeling of Machining Operation* (Vol. 5, pp. 139–148).
- Mathieu, G., Frédéric, V., Vincent, R., & Eric, F. (2015). 3D stationary simulation of a turning operation with an eulerian approach. *Applied Thermal Engineering*, 76, 134–146. <https://doi.org/10.1016/j.applthermaleng.2014.11.049>
- Mondelin, A., Valiorgue, F., Feulvarch, E., Rech, J., & Coret, M. (2013). Calibration of the insert/tool holder thermal contact resistance in stationary 3D turning. *Applied Thermal Engineering*, 55(1–2), 17–25. <https://doi.org/10.1016/j.applthermaleng.2013.02.019>
- Norouzifard, V., & Hamed, M. (2014). Experimental determination of the tool-chip thermal contact conductance in machining process. *International Journal of Machine Tools and Manufacture*, 84, 45–57. <https://doi.org/10.1016/j.ijmachtools.2014.04.006>
- Paula, M. A., Ribeiro, M. V., Souza, J. V. C., & Kondo, M. Y. (2019). Analysis of the performance of coated carbide cutting tools in the machining of martensitic stainless steel AISI 410 in dry and MQL conditions. *Materials Research Express*, 6, 1–12. <https://doi.org/10.1088/2053-1591/ab32a3>
- Polozine, A., & Schaeffer, L. (2005). Exact and approximate methods for determining the thermal parameters of the forging process. *Journal of Materials Processing Technology*, 170, 611–615. <https://doi.org/10.1016/j.jmatprotec.2005.06.017>
- Song, W., Wang, Z., Deng, J., Zhou, K., Wang, S., & Guo, Z. (2017). Cutting temperature analysis and experiment of Ti–MoS₂/Zr-coated cemented carbide tool. *International Journal of Advanced Manufacturing Technology*, 93(1–4), 799–809. <https://doi.org/10.1007/s00170-017-0532-y>
- Tönshoff, H. K., Arendt, C., & Ben Anor, R. (2000). Cutting of hardened steel. *CIRP Annals*, 49(2), 547–566. [https://doi.org/10.1016/S0007-8506\(07\)63455-7](https://doi.org/10.1016/S0007-8506(07)63455-7)
- Wang, Y. M., Tian, H., Shen, X. E., Wen, L., Ouyang, J. H., Zhou, Y., Jia, D. C., & Guo, L. X. (2013). An elevated temperature infrared emissivity ceramic coating formed on 2024 aluminum alloy by microarc oxidation. *Ceramics International*, 39, 2869–2875. <https://doi.org/10.1016/j.ceramint.2012.09.068>
- Xian, Y., Zhang, P., Zhai, S., Yuan, P., & Yang, D. (2018). Experimental characterization methods for thermal contact resistance: A review. *Applied Thermal Engineering*, 130, 1530–1548. <https://doi.org/10.1016/j.applthermaleng.2017.11.091>
- Yen, Y. C., Jain, A., & Altan, T. (2004). A finite element analysis of orthogonal machining using different tool edge geometries. *Journal of Materials Processing Technology*, 146(1), 72–81. <https://doi.org/10.1016/j.jmatprotec.2003.09.020>

- Yuste, M., Galindo, R. E., Sánchez, O., Cano, D., Casasola, R., & Albella, J. M. (2010). Correlation between structure and optical properties in low emissivity coatings for solar thermal collectors. *Thin Solid Films*, *518*, 5720–5723. <https://doi.org/10.1016/j.tsf.2010.04.035>
- Zhang, J., & Liu, Z. (2017). Transient and steady-state temperature distribution in monolayer-coated carbide cutting tool. *International Journal of Advanced Manufacturing Technology*, *91*(1–4), 59–67. <https://doi.org/10.1007/s00170-016-9748-8>
- Zhang, J., Liu, Z., & Du, J. (2017). Prediction of cutting temperature distributions on rake face of coated cutting tools. *International Journal of Advanced Manufacturing Technology*, *91*(1–4), 49–57. <https://doi.org/10.1007/s00170-016-9749-7>
- Zhang, J., Meng, X., Du, J., Xiao, G., Chen, Z., Yi, M., & Xu, C. (2021). Modelling and prediction of cutting temperature in the machining of H13 hard steel of transient heat conduction. *Materials*, *14*(12), 3176. <https://doi.org/10.3390/ma14123176>
- Zhang, J., Zhang, G., & Fan, G. (2022). Effects of tool coating materials and coating thickness on cutting temperature distribution with coated tools. *International Journal of Applied Ceramic Technology*, *19*(4), 2276–2284. <https://doi.org/10.1111/ijac.13854>